e-Proceedings of 2nd International Scientific Conference on
Design and Management of Port Coastal and Offshore Works
Thessaloniki, Greece, May 24-27 2023

A new time-dependent irregular wave propagation model

Th. Karambas[1*], A.G. Samaras[2], Ch. Makris[1]

[1]Department of Civil Engineering, Aristotle University of Thessaloniki, University Campus, 54124 Thessaloniki, Greece
[2]Department of Civil Engineering, Democritus University of Thrace, University Campus - Kimmeria, 67100 Xanthi, Greece
[*]Corresponding author: karambas@civil.auth.gr

Abstract

In this paper a time-dependent numerical model for the simulation of irregular multidirectional wave propagation and transformation in coastal areas, around and inside ports and harbours is presented. The model is capable of simulating the transformation of complex wave fields including shoaling, refraction, diffraction, total and partial reflection from structures, energy dissipation due to wave breaking and bottom friction in a combined way.

Keywords Wave model, Mild slope equation, Irregular waves, Port structures.

1 INTRODUCTION

The simulation of the propagation of multidirectional irregular waves (e.g., estimated by linear superposition of regular waves) in nearshore areas and inside harbours is fundamental for the design of coastal structures. Relevant models should be able to simulate not only the combined wave phenomena but also their interaction with coastal structures (e.g., diffraction, total and partial reflection, etc.) around and inside port basins (Makris et al. 2021).

2 THE 2DH MODEL

The model equations are expressed in terms of the surface elevation and the mean over the depth velocities. A wave spectrum is decomposed in N monochromatic waves. The model consists of the following pair of equations:

$$\frac{\partial \eta_i}{\partial t} + \frac{c_i}{c_{ig}} \nabla \frac{c_{ig}}{c_i} \mathbf{Q}_i = 0 \tag{1}$$

$$\frac{\partial \mathbf{U}_i}{\partial t} + \frac{c_i^2}{d} \nabla \eta_i = \nu_h \nabla^2 \mathbf{U}_i \tag{2}$$

where η_i is the free surface elevation, $\mathbf{U_i}$ the mean velocity vector $\mathbf{U_i} = (U_i, V_i)$, d the depth, $\mathbf{Q_i} = \mathbf{U_y}\, d$, c_i the celerity, c_{ig} the group velocity, and ν_h is a horizontal eddy viscosity coefficient for the simulation of wave breaking. The subscript i denotes the i-th wave component. The right-hand side term of equation (2) is introduced to include breaking effects (Makris et al. 2019, 2021).

Equations (1) and (2) are solved N times separately for each wave component i. Each time step the surface elevation and the horizontal velocities are calculated from the sum of each wave component (Luo et al. 2020):

$$\eta = \sum_{i=1}^{N} \eta_i, \quad U = \sum_{i=1}^{N} U_i, \quad V = \sum_{i=1}^{N} V_i \tag{3}$$

The eddy viscosity coefficient is given by (Karambas and Samaras 2017):

$$\nu_h = 2d \left(\frac{D}{\rho} \right)^{1/3} \tag{4}$$

In Equation (4), D is the dissipation of wave energy expressed as:

$$D = \frac{1}{4} Q_b f \rho g H_m^2 \tag{5}$$

where H_m is the maximum wave height, ρ the water density, f the wave frequency, and Q_b the probability for a wave to break at a depth, expressed as $(1\text{-}Q_b)/(\ln Q_b) = (H_{rms}/H_m)^2$ according to Battjes and Janssen (1978). The mean square wave height H_{rms} is calculated from $H_{rms} = 2(<2\eta^2>)^{1/2}$, with the brackets denoting a time-mean quantity (Makris et al. 2019, 2021).

3 REPRESENTATIONS OF WAVE AND RUBBLE-MOUND BREAKWATER INTERACTION AND SIMULATION OF PARTIAL REFLECTION

The energy loss due to friction effects and due to wave breaking on the slope of rubble mound breakwaters can be represented by inserting an eddy viscosity area in the computational domain instead of the structure geometry, as shown in Figure 1. This approach is based on the premise that knowing the reflection coefficient (e.g., from empirical formulae) one can calculate the value of the eddy viscosity ν_γ introduced in the momentum equation (i.e., Eq. 2 in the previous).

According to Karambas and Bowers (1996) the eddy viscosity coefficient can be calculated by solving the following equations:

$$C_r = \left(\frac{K}{k}\left(1+e^{-4iKS_w}\right) - \left(1-e^{-4iKS_w}\right) \Big/ \frac{K}{k}\left(1+e^{-4iKS_w}\right) + \left(1-e^{-4iKS_w}\right) \right) \qquad \omega^2 - \nu_\gamma \, i \, \omega K^2 = c^2 K^2 \qquad (6)$$

where K is a complex wave number, ω is the radian frequency, c is the wave celerity, $2S_w$ is the length of the area of application of the eddy viscosity coefficient ν_γ. By solving the above equations by iteration, for a given value of the reflection coefficient C_r, the value of the eddy viscosity coefficient ν_γ is obtained (Chondros et al. 2021). The reflection coefficient is given by empirical formulae (e.g., Zanuttigh and van der Meer 2007) as a function of the wave and breakwater characteristics (wave height and period, structure slope, permeability, etc.).

Figure 2 shows an exemplary result of this approach's implementation, presenting the partial wave reflection in front of a breakwater.

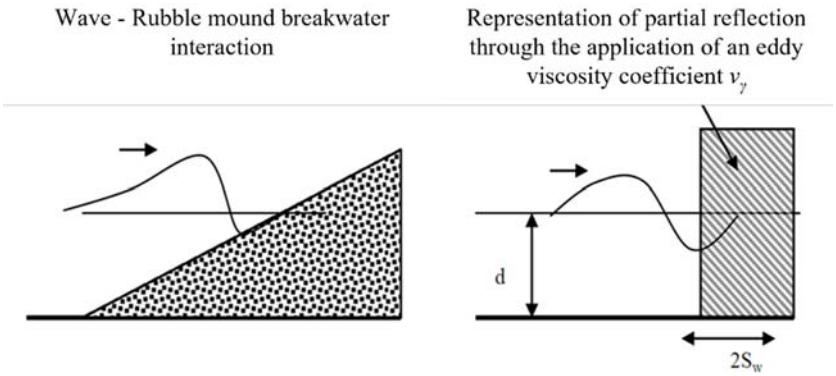

Figure 1. Realistic breakwater and representation in the model by inserting an eddy viscosity area

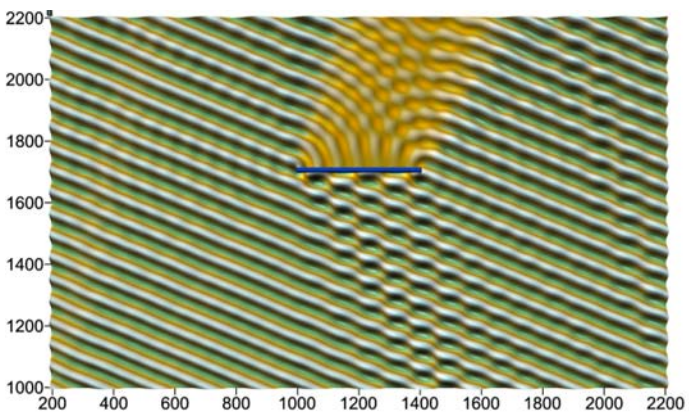

Figure 2. Partial wave reflection from a breakwater

4 MODEL APPLICATIONS AND RESULTS

Firstly, the model is applied to simulate irregular wave propagation over an elliptical shoal, reproducing the Vincent and Briggs (1989) experiments. The experimental layout and a snapshot of free surface elevation in the model's computational domain are presented in Figure 2. Wave transformation in this case is mainly due to bathymetric effects (refraction and bottom diffraction). Figure 3 shows the comparison of model results for unidirectional spectral waves against the experimental data of Vincent and Briggs (1989) along transect No. 4, which lies behind the shoal (test U3, incident significant wave height H_i = 0.0254 m, peak period T_p = 1.3 s). The comparison shows a good agreement between model results and experimental data.

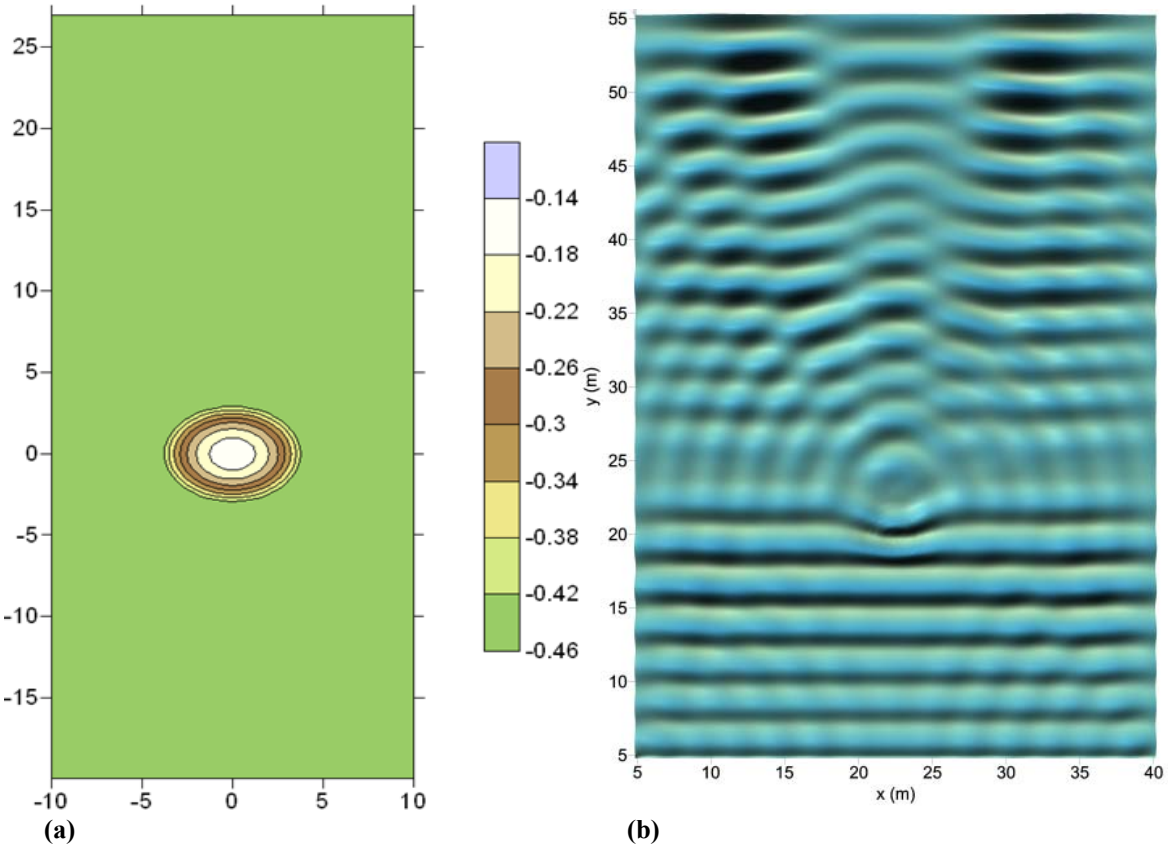

Figure 2. (a) Bathymetry (experimental layout) and (b) snapshot of surface elevation (model computation domain)

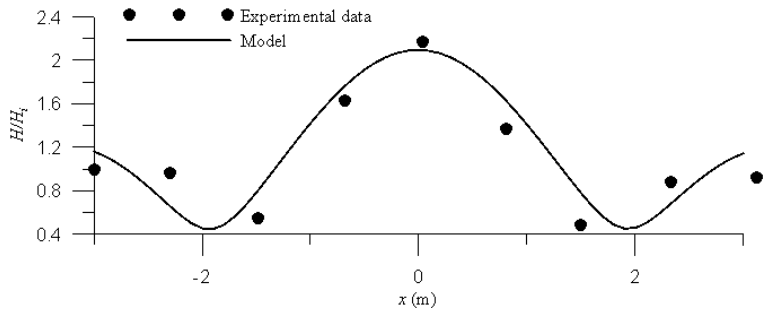

Figure 3. Comparison of model results against the experimental data of Vincent and Briggs (1989), in terms of normalized wave height H/H_i, for spectral unidirectional waves

The second set of numerical experiments concern diffraction of irregular waves passing through a breakwater gap (Li et al. 2000). The incident significant wave height for the case of unidirectional irregular waves is H_s = 0.05 m, the peak period is T_p = 1.20 s and the incident wave angle is equal to 45°. Figure 3 shows model results for the case of gap width B = 3.92 m and B/L = 2 (wave length L

corresponds to the peak period for irregular waves), in the form of a free surface elevation snapshot highlighting the diffraction effects on the irregular waves passing through the gap (left panel) and the diffraction coefficient field behind the breakwater (right panel). Figure 5 shows comparison of model results against experimental data regarding the cross-section distribution of the diffraction coefficients at a distance $y = 3L$ from the breakwater. The agreement in this second case is, again, quite satisfactory.

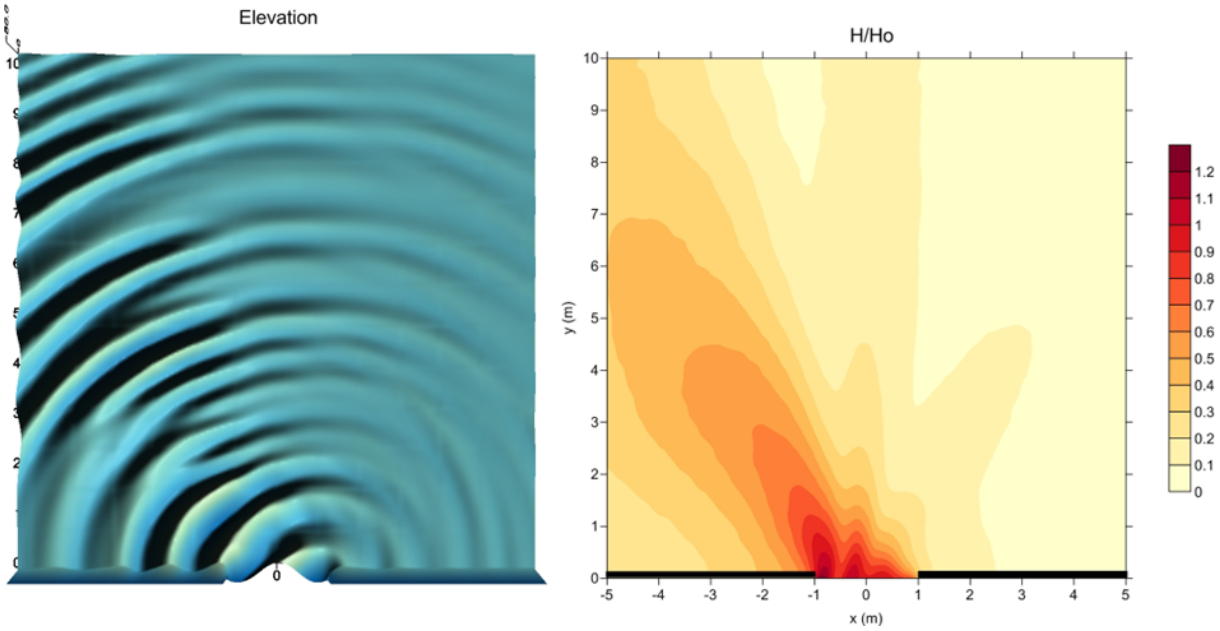

Figure 4. Diffraction of irregular waves passing through a breakwater gap: Free surface elevation snapshot (left panel) and diffraction coefficient field (right panel)

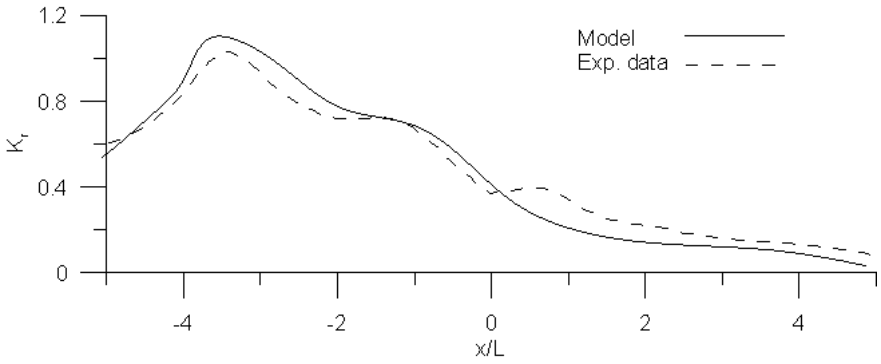

Figure 5. Diffraction of irregular waves passing through a breakwater gap: Comparison of diffraction coefficients K_D at a distance $Y = 3L$ from the breakwater between model results and the experimental data of Li et al. (2000)

Finally, the model is also applied to the real-life harbour layout of the Port of Thessaloniki (Makris et al. 2021). Indicative results for the case of South irregular waves are presented in Figure 5, as a snapshot of free surface elevation, highlighting wave-structure interactions in the harbour area. Comparisons conducted between the proposed model and a simplified mild-slope model have shown differences in wave height distribution that are considered as insignificant; in-depth analysis of this aspect will be included in future versions of this work.

5 CONCLUSIONS

This work presents an evolved version of a formerly presented time-dependent numerical model (Karambas and Samaras 2017; Makris et al. 2019) for the simulation of irregular multi-directional wave propagation and transformation in coastal areas, around and inside ports and harbours. The model is

successfully applied for wave propagation over varying topographies, behind breakwaters as well as in complicated bathymetry setups. The model is proven capable of simulating in an accurate and efficient manner the propagation of irregular waves over any finite water depth in two horizontal dimensions in the presence of coastal structures, including total and partial reflection effects.

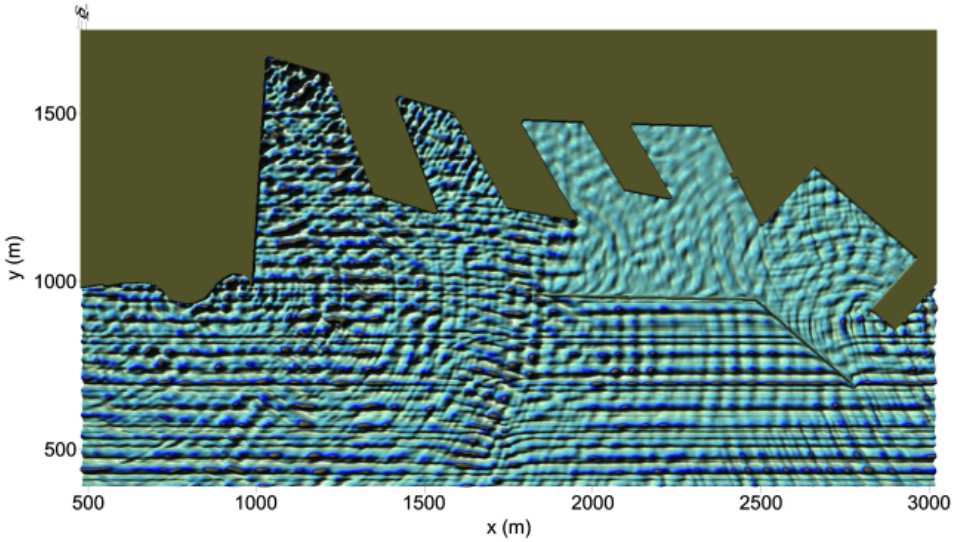

Figure 5. Model results for the Thessaloniki harbour layout: Snapshot of free surface elevation for the case of South irregular waves

References

Battjes JA, Janssen, JPFM (1978) Energy loss and set-up due to breaking of random waves. Paper presented at the 16th International Conference on Coastal Engineering. doi:10.1061/9780872621909.03

Chondros MK, Malliouri DI, Metallinos AS, Papadimitriou AG, Klonaris G, Karambas TV, Makris CV, Baltikas VN, Kontos YN, Nagkoulis N, Tsoukala V, Memos CD (2021) Numerical Modelling of Wave Reflection from Coastal Structures for Reliable Forecasting of Port Downtime. Paper presented at the 17th International Conference on Environmental Science and Technology (CEST2021), Athens, Greece.

Karambas ThV, Bowers EC (1996) Representation of partial wave reflection and transmission for rubble mound coastal structures. Wit Trans Ecol Envir, 12: 415-423. doi:10.2495/HY960421

Karambas ThV, Samaras AG (2017) An Integrated Numerical Model for the Design of Coastal Protection Structures, J Mar Sci Eng, 5:50. doi:10.3390/jmse5040050

Li YS, Liu S-X, Yu X-Y, Lai G-Z (2000) Numerical modeling of multi-directional irregular waves through breakwaters. Appl Math Model, 24(8-9):551-574. doi:10.1016/S0307-904X(00)00003-2

Luo L, Liu S, Li J, Jia W (2020) Deterministic reconstruction and reproduction of multi-directional irregular waves based on linear summation model. Ocean Eng, 198:106952. doi:10.1016/j.oceaneng.2020.106952

Makris C, Androulidakis Y, Karambas T, Papadimitriou A, Metallinos A, Kontos Y, Baltikas V, Chondros M, Krestenitis Y, Tsoukala V, Memos C (2021). Integrated modelling of sea-state forecasts for safe navigation and operational management in ports: Application in the Mediterranean Sea. Appl Math Mod, 89(2):1206-1234. doi:10.1016/j.apm.2020.08.015

Makris C, Karambas T, Baltikas V, Kontos Y, Metallinos, A., Chondros, M., Tsoukala, V., Memos, C. (2019). WAVE-L: An Integrated Numerical Model for Wave Propagation Forecasting in Harbor Areas. Paper presented at the 1st International Conference DMPCO, Athens, Greece, 1:17-21.

Vincent CL, Briggs MJ (1989) Refraction-diffraction of irregular waves over a mound. J Waterw Port Coast Ocean Eng, 115:269-284. doi:10.1061/(ASCE)0733-950X(1989)115:2(269)

Zanuttigh B, van der Meer J (2007) Wave reflection from coastal structures. Paper presented at the 30th International Conference on Coastal Engineering. doi:10.1142/9789812709554_0364